Supplementary Information

Supplementary Note

The magnitude of R_1 *PRE* is determined by the dipole-dipole interaction between the spins of the unpaired electrons and of a nucleus as described by the Solomon−Bloembergen (SB) equations [1,2]:

$$PRE = \frac{2}{5}\left(\frac{\mu_0}{4\pi}\right)^2 \gamma^2 g^2 \mu_B{}^2 s(s+1) r^{-6} J(\omega) \quad (1)$$

$$J(\omega) = \frac{\tau_c}{1+(\omega\tau_c)^2} \quad (2)$$

where μ_0 is the permeability of vacuum ($4\pi \times 10^{-7}$ m kg s^{-2} A^{-2}), γ is the nuclear gyromagnetic ratio (γ_F =25.166 × 10^{-7}, γ_H =26.752 × 10^{-7}), g is the electron Landé g-factor (-2.0023193), μ_B is the magnetic moment of the free electron (−9.284764 × 10^{-24} J/T), s is the electron spin quantum number (s = 3/2, 1, 1/2, 1/2 for Co^{2+}, Ni^{2+}, Cu^{2+}, and MTSL, respectively), *r* is the distance between the electron and the nucleus, and ω is the nuclear Larmor frequency ($4\pi \times 470 \times 10^6$ rad/s for ^{19}F and $4\pi \times 500 \times 10^6$ rad/s for ^{1}H in the instrument we use).

$$\tau_C = (\tau_r{}^{-1} + \tau_S{}^{-1})^{-1} \quad (3)$$

where τ_r is the isotropic protein rotation correlation time and τ_s is electron relaxation time. The τ_s value used for PRE calculation is 3 ps, 132 ps, 4 ns, 100 ns for Co^{2+}, Ni^{2+}, Cu^{2+}, and MTSL, respectively [3-6]. For a protein with hydrodynamic radius *R*, τ_r can be estimated using Stoke's law:

$$\tau_r = \frac{4\pi R^3}{3kT} \quad (4)$$

where k is the Boltzmann constant (1.3806×10^{-23} m^2 kg s^{-2} K^{-1}) and T is the absolute temperature. For a ~300 kDa protein/detergent particle with hydrodynamic radius of 59 Å, as the case for GltPh, we estimate τ_r to be 213 ns.

To take into an account the local motion, we expand the SB equation using the model-free approach as previously described [7-9]:

$$PRE_{MF} = \frac{2}{5}\left(\frac{\mu_0}{4\pi}\right)^2 \gamma^2 g^2 {\mu_B}^2 s(s+1) r^{-6} J_{MF}(\omega) \quad (5)$$

$$J_{MF}(\omega) = \frac{S^2\tau_c}{1+(\omega\tau_c)^2} + \frac{(1-S^2)\tau_t}{1+(\omega\tau_t)^2} \quad (6)$$

$$\tau_t = ({\tau_r}^{-1} + {\tau_s}^{-1} + {\tau_i}^{-1})^{-1} \quad (7)$$

τ_i is the internal correlation time of the ^{19}F label and S^2 is the order parameter. For TET label, we use τ_i of 20 ps and S^2 of 0.1 measured previously for the methionine side chain [10,11] as an approximation.

To estimate the effect of the chemical exchange on the paramagnetic R_1 relaxation, we consider a spin in chemical exchange between a state A with strong PRE and a state B with weak PRE:

$$A \underset{k_{BA}}{\overset{k_{AB}}{\rightleftharpoons}} B \quad (8)$$

The time evolution of the longitudinal magnetizations for the two states, $M_{Z,A}$ and $M_{Z,B}$ is described by the modified McConnell equations [12], which are provided below for clarity:

$$\frac{d(M_{Z,A}-M_{Z,A}^0)}{dt} = -\left(R_{1,A}^* + k_{AB}\right)\left(M_{Z,A} - M_{Z,A}^0\right) + k_{BA}\left(M_{Z,B} - M_{Z,B}^0\right) \quad 9$$

$$\frac{d(M_{Z,B}-M_{Z,B}^0)}{dt} = -\left(R_{1,B}^* + k_{BA}\right)\left(M_{Z,B} - M_{Z,B}^0\right) + k_{AB}\left(M_{Z,A} - M_{Z,A}^0\right) \quad 10$$

where $M^0_{Z,A}$ and $M^0_{Z,B}$ are the magnetizations at time 0 for states A and B, respectively, and $R^*_{1,A}$ and $R^*_{1,B}$ are the intrinsic relaxation rates of the spins in these states. For an inversion recovery experiment, under the initial condition $M_{Z,A}(t=0) = -M_{Z,A}^0$ and $M_{Z,B}(t=0) = -M_{Z,B}^0$ the solutions are:

$$M_{Z,A}(t) = -2\left[M_{Z,AA}^0 exp\left(-R_{1,A}t\right) + M_{Z,AB}^0 exp\left(-R_{1,B}t\right)\right] + M_{Z,A}^0 \quad 11$$

$$M_{Z,B}(t) = -2\left[M_{Z,BB}^0 exp\left(-R_{1,B}t\right) + M_{Z,BA}^0 exp\left(-R_{1,A}t\right)\right] + M_{Z,B}^0 \quad 12$$

Note that

$$M_{Z,A}^0 = f_A M_Z^0 = M_{Z,AA}^0 + M_{Z,AB}^0 \quad 13$$

$$M_{Z,B}^0 = f_B M_Z^0 = M_{Z,BB}^0 + M_{Z,BA}^0 \quad 14$$

where

$M_{Z,A}^0 + M_{Z,B}^0 = M_Z^0$, is the total initial magnetization

and the coefficients $M_{Z,AA}^0$, $M_{Z,AB}^0$, $M_{Z,BB}^0$, $M_{Z,BA}^0$, $M_{Z,A}^0$ and $M_{Z,B}^0$ are:

$$M_{Z,AA}^0 = M_Z^0 \frac{\left[\left(R_{1,A}-D_B\right)f_A + k_{BA}f_B\right]}{E} \quad 15$$

$$M_{Z,AB}^0 = M_Z^0 \frac{\left[\left(-R_{1,B}+D_B\right)f_A - k_{BA}f_B\right]}{E} \quad 16$$

$$M_{Z,BB}^0 = M_Z^0 \frac{\left[\left(-R_{1,B}+D_A\right)f_B + k_{BA}f_B\right]}{E} \quad 17$$

$$M_{Z,BA}^{0} = M_{Z}^{0}\frac{[(R_{1,A}-D_A)f_B-k_{BA}f_B]}{E} \quad 18$$

,f_A and f_B are equilibrium fractions of states A and B. $R_{1,A}$ and $R_{1,B}$ are relaxation rates of the fast and slow phase of the longitudinal relaxation curve in the presence of the chemical exchange, respectively, [12,13]. They depend on the equilibrium fractions of states A and B, on the transition rate k_{BA}, and on the intrinsic relaxation rates of the spin, $R^*_{1,A}$ and $R^*_{1,B}$:

$$R_{1,A} = \frac{D+E}{2} \quad 19$$

$$R_{1,B} = \frac{D-E}{2} \quad 20$$

where

$$D = D_A + D_B = \left(R_{1,A}^{*} + \frac{f_B}{f_A}k_{BA}\right) + \left(R_{1,B}^{*} + k_{BA}\right) \quad 21$$

$$E = \sqrt[2]{\left(R_{1,A}^{*} + \frac{f_B}{f_A}k_{BA} - R_{1,B}^{*} - k_{BA}\right)^2 + 4\frac{f_B}{f_A}k_{BA}^2} \quad 22$$

The intrinsic relaxation rates $R^{*}_{1,A}$ and $R^{*}_{1,B}$, are measured separately in the presence of the blocker, and the values of f_A and f_B are obtained by integrating deconvoluted peaks in 1D ^{19}F-NMR spectra. Therefore, fitting $R_{1,B}$ relaxation curves for spin B to equation 12 requires optimization of only two parameters: k_{BA} and M_Z^0.

Notably, if exchange is very slow, (i.e., $k_{ex} \ll R_{1,A}^{*}$), $M_{Z,AB}^{0} \approx 0$ and $M_{Z,BA}^{0} \approx 0$ the R_1 relaxation becomes mono-exponential:

$$M_{Z,A}(t) = M_{Z,A}^{0}\left[1 - 2exp\left(-R_{1,A}t\right)\right] \quad 23$$

$$M_{Z,B}(t) = M_{Z,B}^{0}\left[1 - 2exp\left(-R_{1,B}t\right)\right] \quad 24$$

i.e. spins in states A and B relax with rate $R_{1,A}$ and $R_{1,B}$, respectively.

In the case of the fast exchange, (i.e., $k_{ex} \gg R_{1,A}^{*} - R_{1,B}^{*}$) [14], $M_{Z,AA}^{0} \approx$, $M_{Z,BA}^{0} \approx 0$, and states A and B relax with the same rate $R_{1,B}$, and

$$R_{1,B} \approx f_A R_{1,A}^{*} + f_B R_{1,B}^{*} \quad 25$$

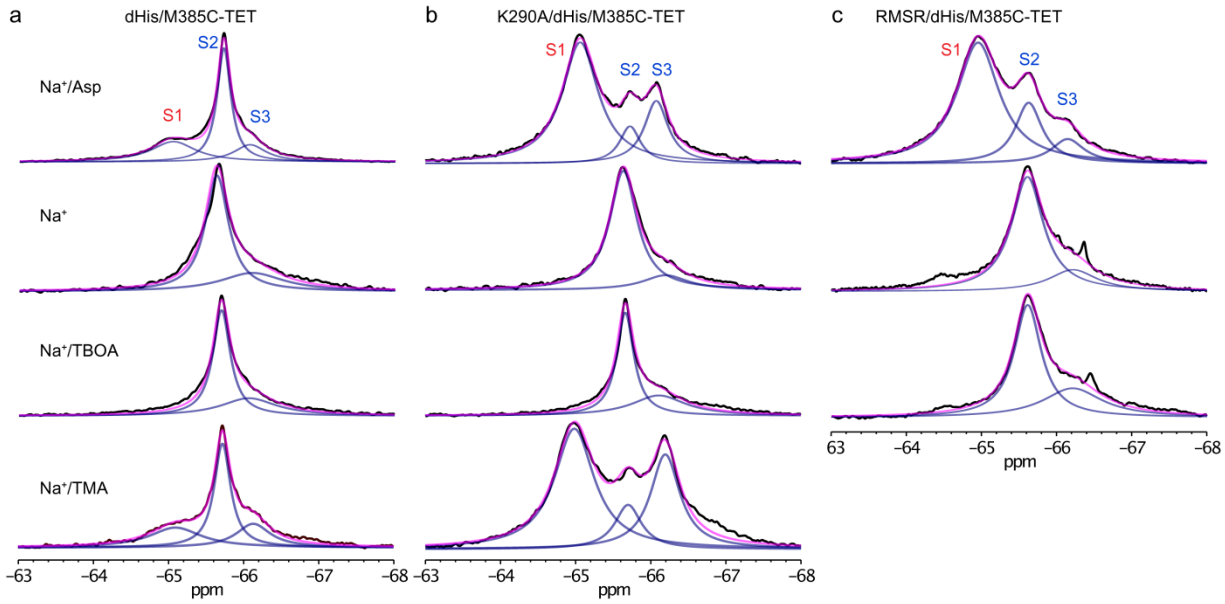

Supplementary Fig. 1. ^{19}F-NMR spectra of TET-labeled GltPh variants bound to different ligand. (**a**), dHis/M385C-TET, (**b**), K290A/dHis/M385C-TET, (**c**), RSMR/dHis/M385C-TET. Experimental conditions from top to bottom are: 200 mM Na^+ and 10 µM L-asp, 0.6 M Na^+ only, 200 mM Na^+ and 1 mM TBOA and 200 mM Na^+ and 1.2 eq. TMA, respectively. All spectra were recorded at 293K. The spectra were deconvoluted into Lorentzian peaks S1, S2 and S3. Raw data are black, fits are magenta and deconvoluted peaks are blue.

Supplementary Table 1. R_1 relaxation rates and conformational exchange rates for GltPh variants.

	S1	S2	S3	S2/S3
dHis/M385C-TET [a]				
$R_{1,ref,\ Asp}$ (s^{-1})	2.9 ± 0.09	3.0 ± 0.08	2.9 ± 0.14	
$R_{1,Ni,\ Asp}$ (s^{-1})	8.3 ± 0.4	3.8 ± 0.27	3.9 ± 0.3	
PRE_{Asp} (s^{-1})	**5.4 ± 0.4**	**0.7 ± 0.3**	**1.0 ± 0.3**	
$f_{ref,Asp}$ (%)	29.8 ± 1.4	44 ± 3.5	26.2 ± 5.0	
$f_{Ni,Asp}$ (%)	59.9 ± 4.5	22.1 ± 3	17.9 ± 1.8	
$R_{1,ref,\ TMA}$ (s^{-1})	3.0 ± 0.19	3.0 ± 0.14	3.0 ± 0.16	
$R_{1,Ni,\ TMA}$ (s^{-1})	9.0 ± 0.4	3.6 ± 0.4	3.5 ± 0.3	
PRE_{TMA} (s^{-1})	**6.0 ± 0.4**	**0.6 ± 0.4**	**0.5 ± 0.4**	
$f_{ref,TMA}$ (%)	27.9 ± 1.5	49.6 ± 2.8	22.5 ± 2.1	
$f_{Ni,TMA}$ (%)	54.4 ± 1.0	32.5 ± 1.0	13.0 ± 1.1	
K290A/dHis/M385C-TET [a]				
$R_{1,ref,\ Asp}$ (s^{-1})	3.0 ± 0.11	2.9 ± 0.14	2.8 ± 0.11	
$R_{1,Ni,\ Asp}$ (s^{-1})	7.3 ± 0.49	5.2 ± 0.45	4.9 ± 0.30	
PRE_{Asp} (s^{-1})	**4.3 ± 0.51**	**2.3 ± 0.47**	**2.1 ± 0.32**	
$f_{ref,Asp}$ (%)	63.3 ± 3.8	12.2 ± 0.8	24.6 ± 2.9	
$f_{Ni,\ Asp}$ (%)	76.2 ± 2.7	13.4 ± 2.6	10.5 ± 2.1	
$R_{1,ref,\ TMA}$ (s^{-1})	3.0 ± 0.13	3.0 ± 0.21	2.9 ± 0.19	
$R_{1,Ni,\ TMA}$ (s^{-1})	8.9 ± 0.2	3.6 ± 0.2	3.5 ± 0.3	
PRE_{TMA} (s^{-1})	**5.9 ± 0.3**	**0.6 ± 0.3**	**0.6 ± 0.4**	
$f_{ref,TMA}$ (%)	56.4 ± 0.4	16.2 ± 1.8	27.5 ± 1.4	
$f_{Ni,\ TMA}$ (%)	77.0 ± 1.9	13.2 ± 2.3	9.8 ± 0.4	
$k_{ex,\ R1,Ni,\ Asp}$ (s^{-1}) [#]		**5.4 ± 2.1[$]**	**3.0 ± 1.2[$]**	
$k_{forward,\ R1,Ni}$ (s^{-1}) [#]		4.6 ± 0.5	2.7 ± 0.3	
$k_{reverse,\ R1,Ni}$ (s^{-1}) [#]		0.75 ± 0.35	0.34 ± 0.04	
$k_{ex,\ EXSY,\ Asp}$ (s^{-1})		1.74 (1.73)	0.79 (1.74)	0.93 (1.13)[†]
$k_{forward,\ EXSY}$ (s^{-1})		1.35 (1.37)	0.67 (1.49)	0.53 (0.69)[†]
$k_{reverse,\ EXSY}$ (s^{-1})		0.36 (0.36)	0.55 (0.14)	0.41 (0.44)[†]
$k_{ex,\ EXSY,\ TMA}$ (s^{-1})				1.23 (1.63)[‡]
$k_{CB,\ EXSY}$ (s^{-1})				0.41(0.60)[‡]
$k_{BC,\ EXSY}$ (s^{-1})				0.82 (1.03)[‡]
RSMR/dHis/M385C-TET [a]				
$R_{1,ref,\ Asp}$ (s^{-1})	3.0 ± 0.07	3.0 ± 0.17	2.9 ± 0.08	
$R_{1,Ni,\ Asp}$ (s^{-1})	8.1 ± 0.4	5.4 ± 0.4	4.5 ± 0.6	
PRE_{Asp} (s^{-1})	**5.1 ± 0.4**	**2.4 ± 0.4**	**1.5 ± 0.7**	
$f_{ref,Asp}$ (%)	67.3 ± 2.6	22.7 ± 2.2	10.0 ± 0.7	
$f_{Ni,\ Asp}$ (%)	83.7 ± 0.9	11.5 ± 0.8	4.9 ± 0.1	
$k_{ex,\ R1,Ni\ Asp}$ (s^{-1}) [#]		**7.1 ± 2.6[$]**	**1.9 ± 1.6[$]**	
$k_{forward,\ R1,Ni}$ (s^{-1}) [#]		6.2 ± 2.6	1.8 ± 1.6	
$k_{reverse,\ R1,Ni}$ (s^{-1}) [#]		0.9 ± 0.4	0.1 ± 0.1	
$k_{ex,\ EXSY,\ Asp}$ (s^{-1})		5.5 (4.58)		

$k_{forward,\ EXSY}$ (s^{-1})		1.7 (1.62)		
$k_{reverse,\ EXSY}$ (s^{-1})		3.8 (2.96)		
$k_{ex,\ STD,\ Asp}$ (s^{-1})			0.77 (0.44)	
$K_{forward,\ STD}$ (s^{-1})			0.67 (0.38)	
$k_{reverse,\ STD}$ (s^{-1})			0.10 (0.05)	
dHis/A381C-TET [b]				
	S1	S2	S3	S0
$R_{1,ref,\ TMA}$ (s^{-1})	2.3 ± 0.08 (2.5 ± 0.1)	2.6 ± 0.03 (2.5 ± 0.1)	2.9 ± 0.1 (2.7 ± 0.1)	2.5 ± 0.3 (3.3 ± 0.4)
$R_{1,Ni,\ TMA,fast}$ (s^{-1})	97.5 ± 5.4 (123.1 ± 14)			124.7 ± 32.0 (133.3 ± 28.5)
$R_{1,Ni,\ TMA,slow}$ (s^{-1})	2.8 ± 0.5 (3.3 ± 0.2)	3.3 + 0.23 (5.4 ± 0.8)	4.5 + 0.5 (4.7 + 0.2)	2.2 ± 1.7 (5.0 ± 1.4)
PRE_{TMA} (s^{-1})	**95.2 (120.6)**	**0.7 (2.8)**	**1.6 (2.0)**	**122.2 (130)**
$f_{ref,TMA}$ (%)	19.9 (17.6)	59.4 (64.4)	16.0 (14.3)	4.9 (4.1)
$f_{Ni,\ TMA}$ (%)	56.8 (53.6)	24.4 (25.2)	12.0 (15.2)	6.8 (6.0)

[#] Rates estimated by fitting the T_1 relaxation curve in the presence of Ni^{2+} ion using equation 12;
[$] Exchange rates between S1 peak and S2 peak and between S1 peak and S3 peak;
[†] Rates k_{ex}, k_{CB} and k_{BC} of K290A/dHis/M385C-TET between S2 and S3 peaks in the presence of Na^+ and Asp;
[‡] Rates k_{ex}, k_{CB} and k_{BC} of K290A/dHis/M385C-TET between S2 and S3 peaks in the presence of Na^+ and TMA;
[a] Data shown are means ± s.d. from 3 independent samples; if the fitting error is larger than s.d. then we report the fitting error; EXSY data in the parentheses are values from a repeat experiment with a independent sample; STD data in the parentheses are values from a repeat experiment with an independent sample;
[b] Errors are the fitting errors. Data in the parentheses are values from a repeat experiment with an independent sample.

Supplementary Table 2. Cryo-EM data collection, refinement and validation statistics

	GltPh OFS (EMD-20922) (PDB 6UWF)	GltPh iOFS (EMD-20923) (PDB 6UWL)
Data collection and processing		
Magnification	81,000	81,000
Voltage (kV)	300	300
Electron exposure (e–/Å^2)	50.1615	50.1615
Defocus range (μm)	-1.5 to -2.5	-1.5 to -2.5
Pixel size (Å)	0.53	0.53
Symmetry imposed	C1	C1
Initial particle images (no.)	2,694,050	2,694,050
Final particle images (no.)	94,731	120,282
Map resolution (Å)	3.08	3.62
FSC threshold	0.143	0.143
Map resolution range (Å)	2.4-3.2	3.0-4.0
Refinement		
Initial model used (PDB code)	2NWX	3V8G
Model resolution (Å)	3.2	3.9
FSC threshold	0.5	0.5
Model resolution range (Å)	3.1-20	3.6-20
Map sharpening *B* factor (Å^2)	-104.1	-146.6
Model composition		
Non-hydrogen atoms	3178	3029
Protein residues	417	402
Ligands	3	2
B factors (Å^2)		
Protein	58.75	30.17
Ligand	67.27	63.10
R.m.s. deviations		
Bond lengths (Å)	0.005	0.007
Bond angles (°)	0.842	1.044
Validation		
MolProbity score	1.22	1.77
Clashscore	2.44	5.44
Poor rotamers (%)	0	0
Ramachandran plot		
Favored (%)	96.6	92.2
Allowed (%)	3.2	7.6
Disallowed (%)	0	0.25

Supplementary References

1 Solomon, I. Relaxation Processes in a System of Two Spins. *Phys. Rev.* **99**, 559-565 (1955).

2 Bloembergen, N. Proton Relaxation Times in Paramagnetic Solutions. *J Chem. Phys.* **27**, 572-573 (1957).

3 Liu, Z., Gong, Z., Guo, D.-C., Zhang, W.-P. & Tang, C. Subtle Dynamics of holo Glutamine Binding Protein Revealed with a Rigid Paramagnetic Probe. *Biochemistry* **53**, 1403-1409 (2014).

4 Jensen, M. R., Hansen, D. F. & Led, J. J. A general method for determining the electron self-exchange rates of blue copper proteins by longitudinal NMR relaxation. *J. Am. Chem. Soc.* **124**, 4093-4096 (2002).

5 Bertini, I., Luchinat, C., Parigi, G. & Ravera, E. in *NMR of Paramagnetic Molecules (Second Edition)* 175-253 (Elsevier, 2017).

6 Kosen, P. A. *Methods Enzymol.* **177,** 86-121 (1989).

7 Lipari, G. & Szabo, A. Model-free approach to the interpretation of nuclear magnetic resonance relaxation in macromolecules. 1. Theory and range of validity. *J. Am. Chem. Soc.* **104**, 4546-4559 (1982).

8 Lipari, G. & Szabo, A. Model-free approach to the interpretation of nuclear magnetic resonance relaxation in macromolecules. 2. Analysis of experimental results. *J. Am. Chem. Soc.* **104**, 4559-4570 (1982).

9 Clore, G. M. & Iwahara, J. Theory, Practice, and Applications of Paramagnetic Relaxation Enhancement for the Characterization of Transient Low-Population States of Biological Macromolecules and Their Complexes. *Chem. Rev.* **109**, 4108-4139 (2009).

10 Igumenova, T. I., Frederick, K. K. & Wand, A. J. Characterization of the Fast Dynamics of Protein Amino Acid Side Chains Using NMR Relaxation in Solution. *Chem. Rev.* **106**, 1672-1699 (2006).

11 Shapiro, Y. E., Polimeno, A., Freed, J. H. & Meirovitch, E. Methyl Dynamics of a Ca^{2+}−Calmodulin−Peptide Complex from NMR/SRLS. *J. Phys. Chem. B* **115**, 354-365 (2011).

12 Ichikawa, K. The effect of chemical exchange on energy relaxation processes in nuclear magnetic resonance spectroscopy. *J. Chem. Soc. Faraday Trans.* **82**, 1913-1919 (1986).

13 Hansen, D. F. & Led, J. J. Implications of using approximate Bloch-McConnell equations in NMR analyses of chemically exchanging systems: application to the electron self-exchange of plastocyanin. *J. Magn. Reson.* **163**, 215-227 (2003).

14 McLaughlin, A. C. & Leigh, J. S. Relaxation times in systems with chemical exchange: Approximate solutions for the nondilute case. *J. Magn. Reson.* **9**, 296-304 (1973).